Article

Application of Corn Straw, an Agro-Waste, to Remove Dyes in an Aqueous Medium, Producing Blue or Red Fibers

Andressa dos Santos, Anne R. Sotiles 🔟 and Fauze J. Anaissi *🔟

Chemistry Department, Universidade Estadual do Centro-Oeste, Guarapuava 85040-167, PR, Brazil;
dossantos.andressa@hotmail.com (A.d.S.); anne.sotiles@gmail.com (A.R.S.)
* Correspondence: anaissi@unicentro.br

Abstract: The contaminant dyes that, even at low concentrations, may cause a series of adverse effects in humans and animals, and their removal by adsorption methods using alternative adsorbents as natural fibers, are regarded as a research topic that has become increasingly relevant. In this study, corn straw (CS), an agro-industrial residue, was used to remove dyes. The samples were characterized by ATR-FTIR, SEM-EDS, zeta potential, diffuse spectra, and colorimetry, before and after dye removal. The analyses allowed us to differentiate the morphology of CS after the treatment's fiber on the adsorbent surface. The zeta potential showed a negative surface charge, but the acidic or alkaline treatment affected the surface charge of the sample, influencing the adsorption of cationic or anionic dyes. Adsorption data presented an increased removal when alkaline treatment was applied for the methylene blue (MB; q_{max} = 16.7 mg g^{-1}), and the acid treatment was more effective for the Congo red (CR; q_{max} = 2.13 mg g^{-1}). After color stability tests, it was observed that the anionic dye CR was more easily desorbed due to the surface charge of the adsorbent. Due to the chemical treatment, corn straw proved to be a good sustainable adsorbent for removing anionic or cationic dyes from aqueous media, contributing directly to the objective of sustainable development (#6—drinking water and sanitation) and with SDG numbers 3, 11, 12, 14, and 17.

Keywords: agro-industrial residue; corn straw; wastewater; dyeing artificial; color stability

1. Introduction

Corn is the world's most produced grain, at around 1.2 billion tons per year, more than in any other farming, because it is considered a staple food for a growing world population, as well as being an important component in animal feed [1]. It is considered multipurpose agricultural farming as it is used in consumer items, industrial products, biofuel, processed foods, and is the main ingredient in corn oil, corn starch, and corn syrup [2]. In Brazil, the use of the no-tillage farming system for this and other crops has increased significantly, as it consists of depositing plant residues on the soil surface, showing profits, and protecting the environment [3]. After the grain harvest, a large amount of dry straw (straw, stalks, foliage) is generated, which can vary from 2 to 15 tons per hectare [4–7]. Researchers have also identified that excess straw, poorly distributed straw, or uneven micro-relief in the soil, contributes to an increase in pest infestations and an increase in greenhouse gas emissions, as well as a reduction in planting density, which causes uneven emergence and delayed initial development [8,9]

With controlled harvesting, it will be possible to mitigate these drawbacks and also produce new materials or bioenergy [9]. Given the abundance of crops and cereals grown in Brazil, agricultural waste has been evaluated as an alternative biomass for innovating materials with low-cost adsorptive capacity and wide availability [10,11]. Straw has fibers that are composed of a cellulosic structure made up of crystalline and amorphous phases, which in turn are characterized by the diversity of functional groups present in the cell wall, which contains hemicellulose, lignin, and cellulose macromolecules [10,12]. The

high content of lignocellulosic material and the high ash content can easily clog the pores of carbon materials, resulting in a low specific surface area and unfavorable adsorption of pollutants [11]. Pre-treatment methods include enzymatic, physical, chemical, and biological methods that can significantly promote the conversion of biomass into high-value-added products [13,14]. This gives rise to the importance of developing high-performance, low-cost, and sustainable pollutant adsorption/removal materials.

Combined with its relevance in the treatment of wastewater, coming mainly from the textile, paint, paper, leather, and printing industries, it requires greater focus. Recent information indicates that more than 100,000 companies have contributed the most to water pollution, releasing products and dyes into the aquatic environment, damaging the ecosystem of aquatic life and consequently human health, directly affecting sustainable development [14,15]. The direct provision of these dye pollutants to the aquatic environment is highly visible and may, even in low concentration, reduce the penetration of solar light to the extent that it affects the photosynthetic processes of aquatic organisms and the balance of the aquatic ecosystem [16]. Dyes from the azo and phenothiazine group are highly resistant to biodegradation under aerobic conditions and their removal is extremely important to minimize damage to aquatic systems [17,18].

Natural fibers from permanent culture are an excellent alternative for treating wastewater contaminated with dyes or metals. Fibers are widely applicable to the development of composite materials, which aligns with the new logic of sustainable development and enhances the production of environmentally-friendly materials, as well being used as reinforcement for polymers [19,20], ceramic materials [21], or in civil construction [22], and therefore, a way of using artificially colored fibers can be using them to remove dyes. To this purpose, the focus of this idea is based on the sustainable development goals (SDGs), one of whose main objectives is to protect and improve natural resources, which includes improving land health, restoring soil and protecting water, managing shortage, and encouraging reuse and recycling [23]. Thus, articulating an essential need (SDG #6), with diverse demands related to the sustainable development objectives proposed by the United Nations.

Hence, the focus of this work is the use of agro-industrial waste, corn straw, as an alternative adsorbent, to optimize and improve the performance of the dye removal process for the treatment of industrial wastewater, and a study of color stability in the sustainable reuse of fibers containing dyes.

2. Materials and Methods

2.1. Materials

Fresh corn straw (CS) samples were collected a few hours after harvest (sommer/2023), Pinhão City, Paraná, Brazil. The phosphoric acid 85% (H_3PO_4; P.A., Biotec, Cotia, Brazil) and sodium hydroxide (NaOH; P.A., NEON, Suzano/Brazil). The methylene blue, MB ($C_{16}H_{18}ClN_3S$; P.A., NEON, Suzano, Brazil) and Congo red, CR ($C_{32}H_{22}N_6Na_2O_6S_2$; P.A., NEON, Suzano, Brazil) dyes were purchased and used without any prior treatment.

2.2. Treatment CS Fibers

The corn straw fibers were prepared by crushing in an industrial blender (Metvisa, Brusque, Brazil; 1000 W) with room temperature water, filtered, and dried for 24 h at 60 °C. After this period, the fibers were dry-milled and then sieved with a standard filter and therefore, produce corn straw naturally (denoted CS). In the acid treatment of the fibers (CS_{acid}), an acid solution of phosphoric acid (0.1 mol L) was added to the CS fiber in a ratio of 1:30 (m:v) and stirred at room temperature for 1 h. After this period, the fibers were vacuum-filtered and dried in a desiccator for 48 h. In the alkaline treatment (CS_{alk}), the same conditions were carried out using a sodium hydroxide solution (0.1 mol L).

2.3. Characterization of CS Fibers

The fiber samples were characterized by attenuated total reflectance with Fourier transform infrared spectroscopy, ATR-FTIR, using the PerkinElmer Frontier device (MA/USA), with a resolution of 4 cm^{-1}, 64 scans, and frequencies between 4000 and 650 cm^{-1}. Scanning electron microscopy, SEM, images were obtained using a SEM-Vega3 LMU from Tescan (Prague, Czech Republic), and elemental composition was viewed with an energy dispersive spectroscopy, EDS, using Inca X-act standard (Oxford, United Kingdom). The measurement of the zeta potential (ζ) was performed in the ZETASIZER Malvern equipment (Malvern, United Kingdom), NANO ZS90 model, with 1000 ppm solution dispersed from water kept in an ultrasonic bath for 480 s, and pH solutions for the samples were 8.00, 7.60, and 7.90 to CS, CS$_{acid}$ and CS$_{alk}$, respectively.

2.4. Study of Dye Removal by CS Fibers

The adsorption experiments were conducted with 0.1 g of CS fibers in a 50 mL Erlenmeyer flask containing 10 mL of deionized water, under stirring and at room temperature, to disperse the fibers. Aliquots of 1.0 mL of dye (0.1 g L^{-1}) were added to the dispersion, every 5 min, until the minimum coloring of the supernatant was observed, in triplicate. The concentrations were determined by ultraviolet spectroscopy (UV-Vis), using spectrophotometer Shimadzu UV-1800 (Kyoto, Japan), at 664 nm (MB) and 500 nm (CR). The amount of adsorbed dye (q_e) in mg g^{-1}, Equation (1), was calculated between the initial concentration (considering the addition of initial water), C_0, and the final concentration, C_f, in g L^{-1}, using the expression,

$$q_e = \frac{\left(C_0 - C_f\right) V}{w} \tag{1}$$

where V is the volume of the final aqueous solution (L), and w is the mass of the adsorbent (g). Dye removal percentage (%) can be calculated as follows, Equation (2):

$$\% \text{ dye removal} = \frac{\left(C_0 - C_f\right)}{C_0} \times 100 \tag{2}$$

2.5. Characterization of Dye-Pigmented CS Fibers (After Study of Dyes Removal)

The diffuse spectra for solids were obtained in an Ocean Optics spectrophotometer, model USB-2000 (Orlando, FL, USA), equipped with optical fiber, tungsten–halogen, silicon source (350–720 nm), and germanium (720–1050 nm) detectors. Color stability was achieved using materials that obtained a greater specific adsorption capacity for each dye, in this case, the samples CS$_{alk}$/MB and CS$_{acid}$/CV were used. Three solution media were used: 1:20 acetic acid (pH 2), 2 g L^{-1} of the sodium bicarbonate (pH 8), and natural water (pH 5). The tests were carried out using 25 mg of colored straw in 5 mL of solution, at room temperature for 72 h. After these periods, the solid samples were filtered, dried in a desiccator, and then analyzed by colorimetric. The colorimetric analyses of the colored straw before and after the color stability was performed using a portable colorimeter 3nh, model NR60CP (Zhejiang, China) with a D65 light source. In colorimetric (CIEL*a*b*), the total color deviation is expressed by the value of ΔE, which was created by the CIE to designate a metric distance and can be calculated using Equation (3):

$$\Delta E_{ab}^* = \sqrt{\left(L_2^* - L_1^*\right)^2 + \left(a_2^* - a_1^*\right)^2 + \left(b_2^* - b_1^*\right)^2} \tag{3}$$

where ΔL is the light variation, Δa is a parameter variation (green–red), and Δb is the b parameter variation (blue–yellow).

3. Results and Discussion

3.1. Characterization of CS Fibers

3.1.1. ATR-FTIR

Infrared spectra of the corn straw fibers (nature, acid, or alkaline) showed characteristic absorption signals for lignin and cellulose structures, as shown in Figure 1. Lignin is confirmed by the absorption signal at 1730 cm^{-1}, corresponding to C=O carboxyl vibrational stretches [24,25]. In acid treatment processes, the metal ions chemically linked to the carboxyl groups of the biomass are mostly removed, which results in a slight increase in absorbance in this region, relating the carboxyl groups of the uronic acid in the hemicellulose of the pre-treated samples [26]. While the peak at 1514 cm^{-1} is the stretching vibration of the C=C aromatic ring that corresponds to cellulose and lignin, in the alkalization process, the signal intensifies slightly due to the presence of water absorbed by the cellulose [10,24]. Another band-typical structure of cellulose is evidenced at 898 cm^{-1}, which was due to the β-glycosidic bond of the glucose ring, where this sign indicates that the pre-treatments did not completely remove cellulose and sugars present in the straw [12,25].
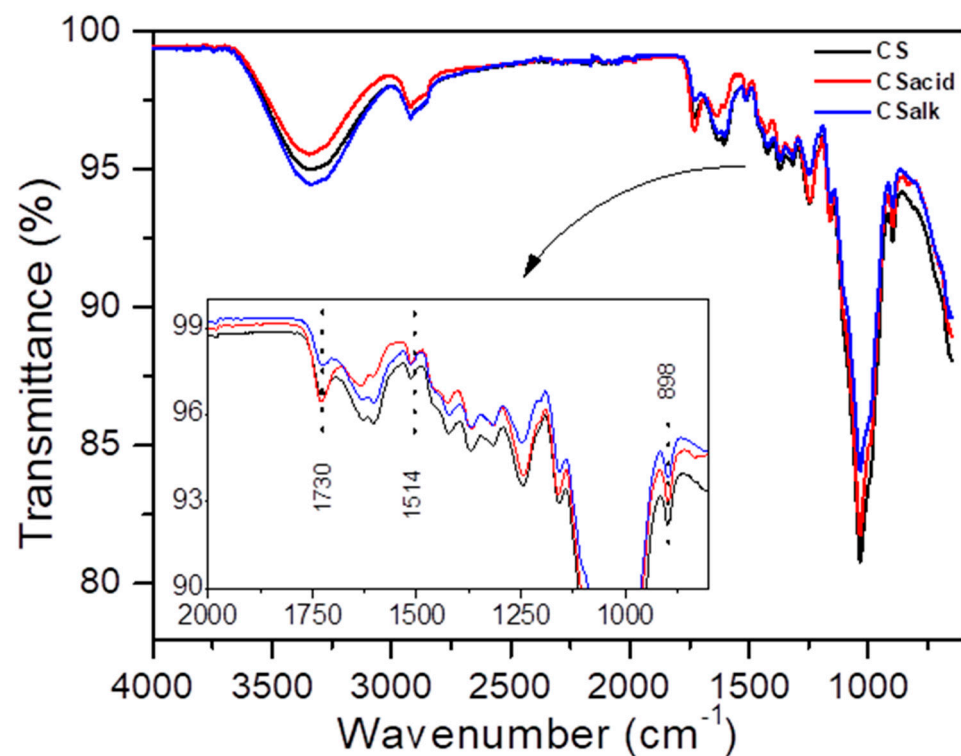

Figure 1. Spectrum ATR-FTIR of the corn straw after and before treatment.

3.1.2. SEM-EDS

The SEM images of the samples are demonstrated in Figure 2. The corn straw surface was smooth and intact, with an organized and compact structure, and the cellulose and hemicellulose were tightly wrapped by lignin before pretreatment (Figure 2a) [12,24]. After acid treatment, the surface became wrinkled and the wrapping structure was broken (Figure 2b) [26]. The same was observed with large voids for the alkaline treatment, moreover, the structure was partially corrupt, resulting in a thin layer of rough surface (Figure 2c) [12,24].
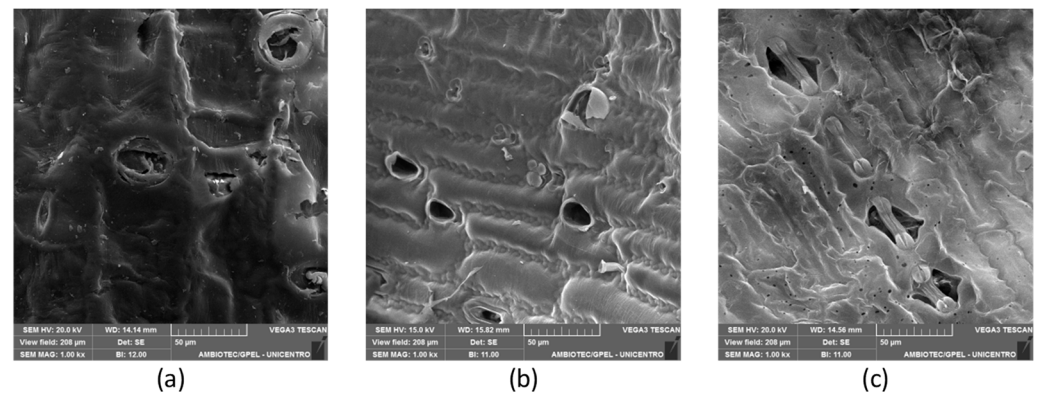
Figure 2. Scanning electron microscope images of the (**a**) CS, (**b**) CS$_{acid}$, and (**c**) CS$_{alk}$.

The action of the treatments lies in the effectiveness of the lignocellulosic structure, depending on the method used, since the attack takes place on different parts of the substrate by different chemical reagents. Acid attack results in the solubilization of hemicellulose and the reduction of cellulose, which occurs by breaking the covalent bonds, hydrogen bonds, and Van der Waals forces that hold the biomass components together [27,28]. In contrast, in alkaline treatment, the lignin and polysaccharide bonds are broken, making the lignocellulose more exposed [27,29].

Table 1 shows the elemental composition of the surface of the corn straw before and after the chemical treatments. The high content of the carbon and oxygen elements in all the samples represents the morphological and structural conservation of the surface of the fibers, providing a high degree of active coordination sites (-COOH and -COO$^-$) [30,31]. The elementary difference in surface morphology is the presence of small stomata and silicon bodies exposed due to the dissolution of lignin and hemicellulose after the treatments [32]. They may be providers of coordination bonds and capture dye molecules of different natures, cationic or anionic [33,34]. Other metallic elements were found on the surface of the CS$_{alk}$, and the element sodium (Na) is present due to the chemical reagent used in the treatment. The presence of metal ions increases the positivity of the species, favoring the formation of ionic bonds between the surface of the fiber and anionic dyes, electrostatic interactions [35].

Table 1. Surface elemental composition analysis by EDS.

Elements	Sample		
	CS (%)	CS$_{acid}$ (%)	CS$_{alk}$ (%)
O	55.59 ($\pm$0.28)	49.99 ($\pm$0.14)	54.47 ($\pm$0.31)
C	41.43 ($\pm$0.29)	49.87 ($\pm$0.14)	43.88 ($\pm$0.32)
Mg	1.11 ($\pm$0.03)	--	0.29 ($\pm$0.02)
K	0.64 ($\pm$0.01)	--	0.24 ($\pm$0.01)
Ca	1.23 ($\pm$0.02)	--	0.25 ($\pm$0.01)
Si	--	0.14 ($\pm$0.01)	0.30 ($\pm$0.02)
Na	--	--	0.57 ($\pm$0.04)

Condition EDS Inca X-act standart with 129 EV resolution.

3.1.3. Zeta Potential

The negative charges of corn straw samples stem mainly from the phenolic hydroxyl and carboxyl groups of lignin, which are negatively charged in an alkaline medium as shown by their respective zeta potentials (Figure 3) [36]. Generally, in acid treatment, H$^+$ interacts with the negative surface of the lignin colloid, making it less negative and increasing particle size, accelerating coagulation [30,36,37]. The decrease in zeta potential on alkaline treatment occurred due to the more effective extraction of soluble lignin in the basic medium, forming lignin colloidal structures with a more negative charge, promoting

electrostatic interactions and thereby keeping a stable solution [38]. The surface charge of the samples was negative, which could have a greater electrostatic attraction effect on the dyes.
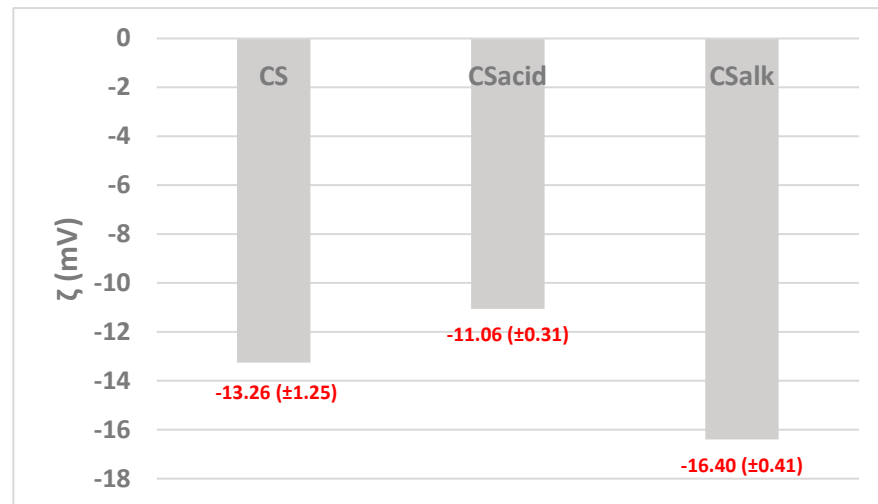

Figure 3. Zeta potential data.

3.2. Dyes Removal Test

Two dyes with opposite charges were used as models for testing the removal excessive amounts, methylene blue and Congo red, a cationic dye and an anionic dye, respectively. As a result, the removal efficiency of all samples was higher for MB, presenting a maximum value of 99.2% with CS_{alk}, while for the removal of CR in CS_{acid} was 77.2%, as shown in Table 2.

Table 2. Percentage of dye removal, amount adsorbed, and removed ration data.

Sample	Methylene Blue		Congo Red		Amount Removed Ration MB/CR (q_e/q_e)
	Removal (%)	q_e (mg g^{-1})	Removal (%)	q_e (mg g^{-1})	
CS	93.5 ($\pm$0.8)	10.8 ($\pm$0.2)	44.2 ($\pm$1.2)	1.37 ($\pm$0.2)	7.88
CS_{acid}	85.2 ($\pm$3.0)	9.80 ($\pm$0.7)	77.2 ($\pm$0.5)	2.13 ($\pm$0.1)	4.60
CS_{alk}	99.2 ($\pm$0.2)	16.7 ($\pm$0.1)	33.9 ($\pm$3.2)	1.05 ($\pm$0.2)	15.9

Condition dye removal in room temperature and under stirring at 500 rpm.

This difference is because the surface has an electrically negative charge and a greater interaction is created for positively charged adsorbates, because of the presence of OH$^-$ ions when treated in an alkaline medium [10,16]. On the other hand, the test using anionic adsorbate was less effective, created by the electrostatic repulsion of the surface of the adsorbent and the CR, but showed some efficiency in the percentage of removal [16]. According to the ratio of the amount removed between the dyes, there is indeed a greater affinity for cationic dyes, but this does not rule out the effectiveness of removing anionic dyes, caused by electrostatic interactions, and the selectivity of the dye was consistent with the zeta potential presented by the samples. The sample with the most negative potential value, CS_{alk} (-16.40 mV), showed better removal for the cationic dye MB, while the sample with the lowest potential value, CS_{acid} (-11.06 mV), was the one that showed better removal for the anionic dye, Congo red.

The surface of CS is rich in hydroxyl groups, providing effective hydrogen bonds with the cationic dye MB, this factor increases the adsorption capacity when alkaline treatment of the fiber is present. In addition, interactions between the coordination sites of the adsorbent (-COOH) and the aromatic rings of MB can occur through hydrophobic interactions of the π-π bond type [30]. The presence of the acid by treatment, increases the positive charge of the surface, favoring the adsorption of the anionic dye CR to the CS_{acid} surface [35]. The

strong interaction is the presence of active coordination groups of the functional groups (-COO$^-$) with the primary amine of the CR dye, forming effective H-bonds [31].

3.3. Characterization of Dyed Corn Straw Fibers

3.3.1. Diffuse Spectra

Figure 4 shows the diffuse spectra of the initial corn straw samples, and those pigmented with the dyes methylene blue (Figure 4a) and Congo red (Figure 4b), in absorbance mode. The absorption spectrum of methylene blue is characterized by intense bands in the 640–850 nm region, it is composed of two maxims at 687 nm and 779 nm. The high peak at 779 nm shows a high quantity of monomers compared to the peak at 687 nm, which suggests a low quantity of dimers. This is due to the high degree of molecular electronic conjugation where hydrophobic interactions occur between the dye rings [38–40]. When MB is adsorbed onto corn straw, the displacement and widening of the bands to the 500–800 nm region indicate the intensification of intermolecular interactions and the electronic coupling of interaction with the straw surface, while also preserving the dye's characteristic color tone [39].
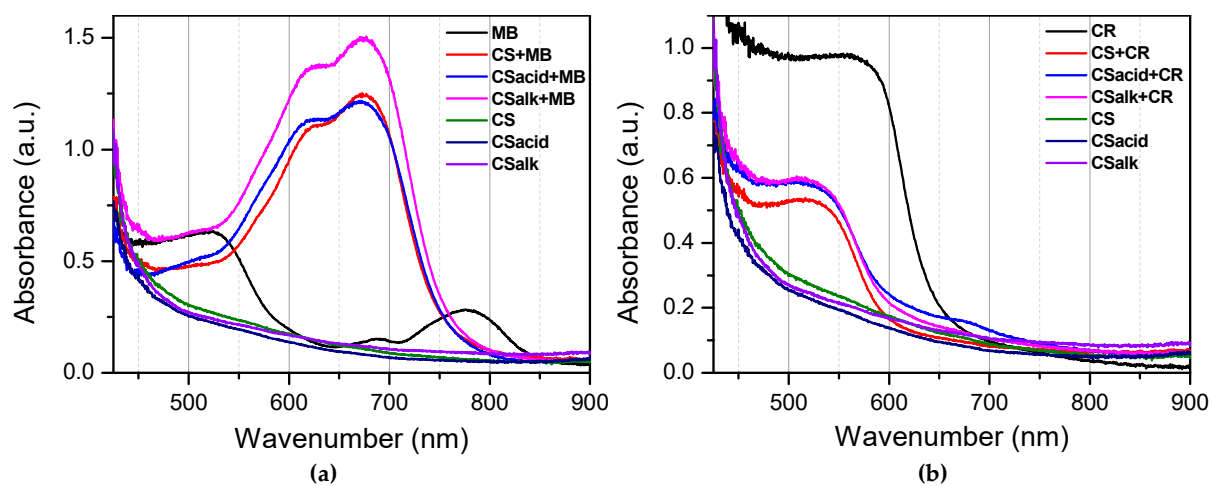

Figure 4. Absorbance spectra of corn straws non-treated and treated with the (**a**) MB removed and (**b**) CR removed.

Congo red has a maximum absorbance of 561 nm, which decreases and changes when it binds to the fibrous material to 516 nm. In addition to the electrostatic interactions already known and mentioned, adsorption of the dye is actively facilitated by hydrogen bonds which depend on functional groups and active coordination sites present on the solid surface [16]. The one strong interaction is the presence of active coordination groups of the functional groups (COO$^-$), formed under synthetic conditions, which can form a strong H-bond with the Congo red-containing primary amine, which will lead to a high adsorption capacity, thus decreasing the electronic conjugation of the dye rings and reducing the wave number in the spectrum [31].

The reflectance spectra were acquired in the 400 to 900 nm range, as shown in Figure 5. In general, the straw samples before and after chemical treatment did not show any gaps and exhibited similar spectral reflectance graphs. However, when the straws contained the dyes, there was a transition jump where their highest light reflectance occurred in the visible range.
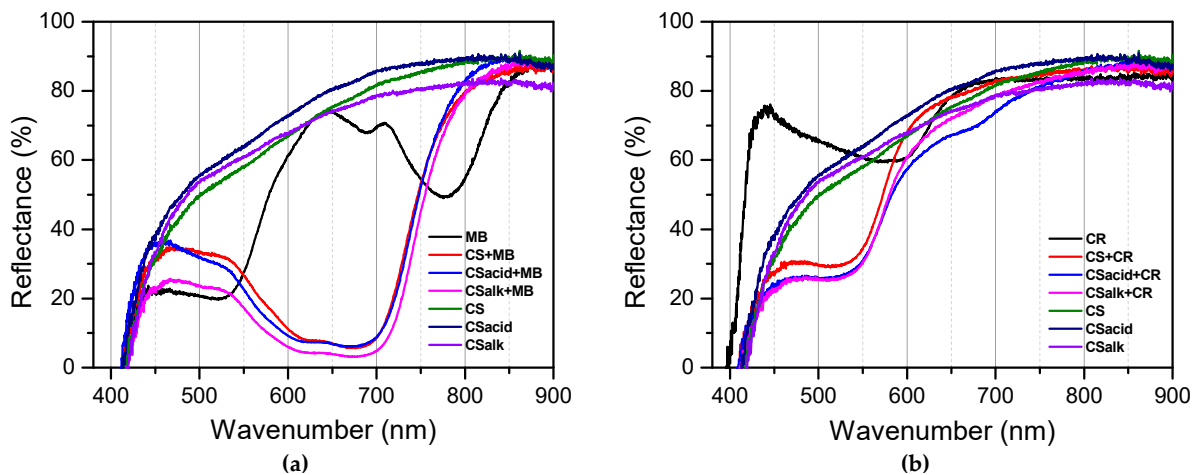
Figure 5. Reflectance spectra of corn straws non-treated and treated with the (**a**) MB removed and (**b**) CR removed.

The Figure 5a, the reflectance mode in the MB-containing samples reached a non-ideal plateau shape, unlike those in the VC-containing samples (Figure 5b). Stronger blue and green pigments with high saturation reflect light at longer wavelengths, starting at 800 nm, and moderate reflectance in the blue–violet region, at 450 nm. Red and yellow pigments, on the other hand, show good reflectance from 600 nm and pass through almost all the red and green bands [41,42]. The fingerprints of colored straws are comprised of the original colors, where part of the visible spectrum is absorbed, and part is reflected by the object. Spectral values alone are not enough to communicate the visual appearance of colors, so we must consider the effect of lighting and how colors are perceived by colorimetry.

3.3.2. Colorimetry

It is possible to observe a visual change in the color of the samples after the dye removal process. When a graph is plotted as a function of the parameters $a*$ (where negative refers to green and positive to red) and $b*$ (where negative refers to blue and positive to yellow) (Figure 6), it is observed that in comparison with natural fibers, when the methylene blue dye is adsorbed, the colorimetric resultant moves towards the negative direction of both $a*$ and $b*$, while when the Congo red dye is adsorbed, the colorimetric resultant moves only towards to the positive axis of $a*$, for redder tones.
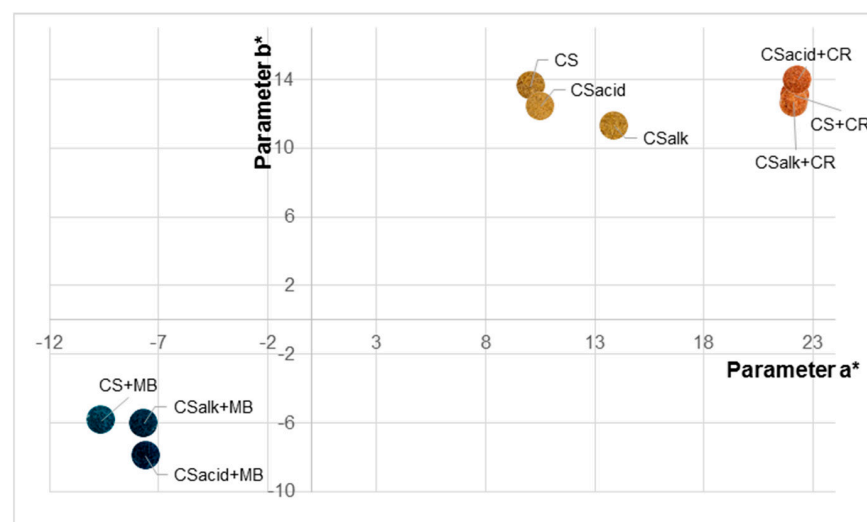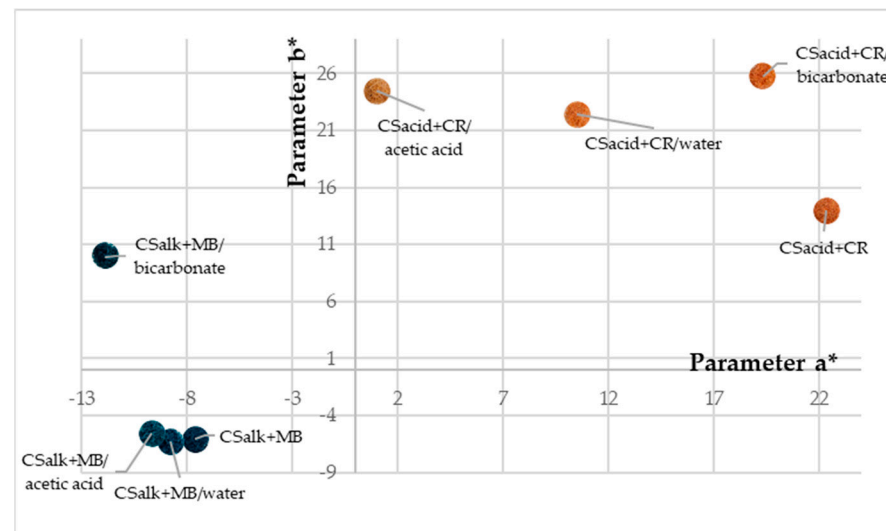

Figure 6. Relationship between the colorimetric parameters $a*$ and $b*$ in the coloring corn straw samples after adsorption with methylene blue and Congo red.

The resulting values for ΔE of all samples are above 12, falling into the category of very strong change in color (Table S1) [43]. Furthermore, the values referring to ΔE are consistent with the adsorption analysis and the percentages of dye removal by the fibers, and the CS_{alk} sample which showed the highest percentage of removal for the methylene blue dye, also showed the greatest difference in color of the fiber without pigment, and the same occurred for the CS_{acid} sample, which presented better results for the Congo red dye.

3.3.3. Chemical Color Stability

The results of the color stability analysis (Figure 7) show that the samples exposed to natural water, acetic acid, and sodium bicarbonate, showed a more significant color shift for CS_{acid}+CR. In parameter a^*, the samples containing CR moved to the left, with the acidic solution being more aggressive, showing greater discoloration of the red color.

Figure 7. Relationship between the colorimetric parameters a^* and b^* in the coloring corn straw samples after desorption with methylene blue and Congo red.

Preference is given to protonation of the primary amines of Congo red molecules in solution, rather than those attached to the CS_{acid} surface [44]. This is different for CS_{alk}+MB, as there was no significant variation in colors, except in sodium bicarbonate medium, increasing brightness (L^*), as shown in Table 3. This factor may be attributed to the fact that sodium bicarbonate can act as a bleaching agent for the fiber, also influencing the lesser loss of color in the case of Congo red [45,46]. It is possible that the greater discoloration of the Congo red dye compared to methylene blue was a result of the surface charge of the fibers, which presented a negative charge and therefore, greater affinity for the cationic dye MB and, consequently, the anionic dye CR would be desorbed more easily.

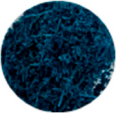**Table 3.** Colorimetry results of the color stability test.

Sample	Colorimetric Parameters *						Photo
	L^*	a^*	b^*	c	h	ΔE	
CS_{alk}+MB	13.32	−7.65	−6.02	9.74	248.20	-	
CS_{alk}+MB/natural water	14.93	−8.78	−6.28	10.31	217.52	3.61	

Table 3. *Cont.*

Sample	Colorimetric Parameters *						Photo
	L *	*a* *	*b* *	c	h	ΔE	
CS$_{alk}$+MB/acetic acid	16.01	−9.66	−5.53	11.13	209.73	3.39	
CS$_{alk}$+MB/sodium bicarbonate	25.01	−11.88	10.03	15.55	139.83	5.90	
CS$_{acid}$+CR	70.31	22.32	13.98	26.34	32.05	-	
CS$_{acid}$+CR/natural water	79.02	10.48	22.42	24.75	64.96	16.95	
CS$_{acid}$+CR/acetic acid	78.42	14.28	24.48	28.34	59.75	15.51	
CS$_{acid}$+CR/sodium bicarbonate	81.67	19.31	25.75	27.38	70.13	16.63	

* Colorimetric analyzes carried out at room temperature with dry straw.

4. Conclusions

In this work, adsorbents from corn straw, a biomass agro-industrial waste, when non-treated and treated with acid and base (CS, CS$_{acid}$, and CS$_{alk}$), were characterized and used in the adsorption performance for cationic (methylene blue) and anionic (Congo red) dyes and their coloration was studied. The studies showed that the alkaline treatment was the most aggressive on the fibers, leaving them with a more negative surface charge, with a rough structure, and exposure of the lignin through digestion of the hemicellulose and cellulose structure. This results in a greater affinity for adsorption of the MB dye, where electrostatic and hydrophobic interactions of the π-π bond type between the surface of the straw alkaline treated environment and the aromatic rings of the dye may be present. For CR dyes, acid treatments on the fiber surface favor their adsorption by sites of coordination groups with primary amines of the dye, forming H-bonds.

After the adsorption process, the dyed fibers showed similar electronic spectra to their original color/dye structure, with a slight shift in the wavenumber when bonded to the fiber surface. This factor may be associated with an electronic rearrangement of the structures of the dyes when attached to the coordination groups on the surface of the straws. A high reflectance, in the visible region, was observed after dyeing the fibers in both shades of color.

The colorimetric analysis was consistent with the adsorption results, and the CS$_{alk}$+MB and CS$_{acid}$+CR samples that adsorbed the most were those with the highest color intensity. In terms of color stability, the anionic dye Congo red was more easily desorbed, possibly due to the negative surface charge of the samples, while the cationic dye was less affected. For both dyes, the bicarbonate medium was appointed to intensify the color due to the bleaching of the fiber. Although the surface charge of the adsorbent affects the adsorption and desorption process, the corn straw proved to be a sustainable and promising adsorbent

for both dye species, which can be exposed to different media and still maintain their color relatively well.

Data Availability Statement: The data used to support the findings of this study are available from the corresponding author upon request.

Conflicts of Interest: The authors declare no conflict of interest.

References

1. Corn Industry Worldwide—Statistics & Facts. Available online: https://www.statista.com/topics/7169/corn-industry-worldwide/ (accessed on 3 January 2024).
2. Shibukawa, V.P.; Reis, C.E.R.; dos Santos, J.C.; Da Rós, P.C.M. Utilization of Co-Products from Corn Ethanol Industry in a Biorefinery Context: A Review on the Biotechnological Potential of Thin Stillage. *Braz. J. Chem. Eng.* **2023**, 17. [CrossRef]
3. Plantio Direto a Palhada Do Bem. Available online: https://www.embrapa.br/contando-ciencia/agricultura/-/asset_publisher/FcDEMJIbvFle/content/plantio-direto-a-plahada-do-bem/1355746?inheritRedirect=false#:~:text=O%20sistema%20de%20plantio%20direto,com%20isso,%20o%20aquecimento%20global (accessed on 24 January 2024).
4. de Barcellos Ferreira, A.C.; Borin, A.L.D.C.; Lamas, F.M.; Sofiatti, V. Cover Plants in Second Crop: Nutrients in Straw and Cotton Yield in Succession. *Pesqui. Agropecuária Trop.* **2023**, *53*, e75032. [CrossRef]
5. Lange, A.; Cabezas, W.A.R.L.; Trivelin, P.C.O. Produtividade de Palha e de Milho No Sistema Semeadura Direta, Em Função Da Época Da Aplicação Do Nitrogênio No Milho. *Rev. Bras. Milho Sorgo* **2009**, *8*, 57–68. [CrossRef]
6. Crespo, A.M.; Souza, M.N.; Favarato, L.F.; Guarçoni, R.C.; Araújo, J.B.S.; Rangel, O.J.P.; de Souza, J.L.; da Costa Gonçalves, D. The Green Corn Development and Yield on Different Summer Soil Covering Plants in the Organic No-Tillage System. *Int. J. Adv. Eng. Res. Sci.* **2022**, *9*, 217–225. [CrossRef]
7. Ruedell, J. Manejo Do Solo e Da Água Nos Sistemas de Produção Da Atualidade e Do Futuro. *Rev. Plantio Direto Tecnol. Agrícola* **2017**, *155*, 36–48.
8. No Plantio Direto o Milho é o Melhor. Available online: https://revistacultivar.com.br/artigos/no-plantio-direto-o-milho-e-o-melhor (accessed on 23 January 2024).
9. Resíduo Da Colheita de Cana, Palha Protege o Solo e Tem Alto Potencial Gerador de Bioenergia. Available online: https://cnpem.br/residuo-da-colheita-de-cana-palha-protege-o-solo-e-tem-alto-potencial-gerador-de-bioenergia-2/ (accessed on 2 February 2024).
10. Değermenci, G.D.; Değermenci, N.; Ayvaoğlu, V.; Durmaz, E.; Çakır, D.; Akan, E. Adsorption of Reactive Dyes on Lignocellulosic Waste; Characterization, Equilibrium, Kinetic and Thermodynamic Studies. *J. Clean. Prod.* **2019**, *225*, 1220–1229. [CrossRef]
11. Ma, P.; Yao, S.; Wang, Z.; Qi, F.; Liu, X. Preparation of Nitrogen-Doped Hierarchical Porous Carbon Aerogels from Agricultural Wastes for Efficient Pollution Adsorption. *Sep. Purif. Technol.* **2023**, *311*, 123250. [CrossRef]
12. Liu, Z.; Li, L.; Liu, C.; Xu, A. Pretreatment of Corn Straw Using the Alkaline Solution of Ionic Liquids. *Bioresour. Technol.* **2018**, *260*, 417–420. [CrossRef]
13. Monlau, F.; Barakat, A.; Trably, E.; Dumas, C.; Steyer, J.; Carrère, H. Lignocellulosic Materials Into Biohydrogen and Biomethane: Impact of Structural Features and Pretreatment. *Crit. Rev. Environ. Sci. Technol.* **2013**, *43*, 260–322. [CrossRef]
14. Hendriks, A.T.W.M.; Zeeman, G. Pretreatments to Enhance the Digestibility of Lignocellulosic Biomass. *Bioresour. Technol.* **2009**, *100*, 10–18. [CrossRef]
15. Mosbah, A.; Chouchane, H.; Abdelwahed, S.; Redissi, A.; Hamdi, M.; Kouidhi, S.; Neifar, M.; Slaheddine Masmoudi, A.; Cherif, A.; Mnif, W. Peptides Fixing Industrial Textile Dyes: A New Biochemical Method in Wastewater Treatment. *J. Chem.* **2019**, *2019*, 5081807. [CrossRef]

16. dos Santos, A.; Viante, M.F.; dos Anjos, P.P.; Naidek, N.; Moises, M.P.; de Castro, E.G.; Downs, A.J.; Almeida, C.A.P. Removal of Astrazon Blue Dye from Aqueous Media by a Low-Cost Adsorbent from Coal Mining. *Desalin. Water Treat.* **2016**, *57*, 27213–27225. [CrossRef]

17. Ranjbari, S.; Ayati, A.; Niknam Shahrak, M.; Tanhaei, B.; Hamidi Tabrizi, S. Design of [BmIm]$_3$PW$_{12}$O$_{40}$ Ionic Liquid Encapsulated-ZIF-8 Nanocomposite for Cationic Dye Adsorptive Removal: Modeling by Response Surface Methodology. *Ind. Eng. Chem. Res.* **2023**, *62*, 4636–4645. [CrossRef]

18. Trentini, J.D.; Jaerger, S.; Balaba, N.; Alves, H.J.; Wypych, F.; Anaissi, F.J. Adsorptive Removal of Congo Red by Macroporous ZnO Obtained from Citrus Pectin Gelation and Reuse as a Hybrid Pigment. *Part. Sci. Technol.* **2023**, *41*, 120–130. [CrossRef]

19. Favaro, S.L.; Ganzerli, T.A.; de Carvalho Neto, A.G.V.; da Silva, O.R.R.F.; Radovanovic, E. Chemical, Morphological and Mechanical Analysis of Sisal Fiber-Reinforced Recycled High-Density Polyethylene Composites. *Express Polym. Lett.* **2010**, *4*, 465–473. [CrossRef]

20. dos Santos, F.D.D.; Batistela, V.R.; dos Santos, A.; Halison de Oliveira, J.; Radovanovic, E.; Granzotto, D.C.T.; Fávaro, S.L. Hybrid Polyurethane/Natural Fibers Composites Optimized by Simplex-Centroid Mixture Design. *J. Compos. Mater.* **2022**, *56*, 1039–1052. [CrossRef]

21. Laverde, V.; Marin, A.; Benjumea, J.M.; Rincón Ortiz, M. Use of Vegetable Fibers as Reinforcements in Cement-Matrix Composite Materials: A Review. *Constr. Build. Mater.* **2022**, *340*, 127729. [CrossRef]

22. Li, V.C. From Micromechanics to Structural Engineering—The Design of Cementitious Composites for Civil Engineering Applications—Review. *Jpn. Society Civ. Eng.* **1993**, *10*, 37s–48s.

23. The 17 Goals—Sustainable Development. Available online: https://sdgs.un.org/goals (accessed on 20 February 2024).

24. Gunam, I.B.W.; Setiyo, Y.; Antara, N.S.; Wijaya, I.M.M.; Arnata, I.W.; Putra, I.W.W.P. Enhanced Delignification of Corn Straw with Alkaline Pretreatment at Mild Temperature. *Rasayan J. Chem.* **2020**, *13*, 1022–1029. [CrossRef]

25. Chen, D.; Gao, D.; Huang, S.; Capareda, S.C.; Liu, X.; Wang, Y.; Zhang, T.; Liu, Y.; Niu, W. Influence of Acid-Washed Pretreatment on the Pyrolysis of Corn Straw: A Study on Characteristics, Kinetics and Bio-Oil Composition. *J. Anal. Appl. Pyrolysis* **2021**, *155*, 105027. [CrossRef]

26. YANG, C.; LU, X.; LIN, W.; YANG, X.; YAO, J. TG-FTIR Study on Corn Straw Pyrolysis-Influence of Minerals. *Chem. Res. Chinese Univ.* **2006**, *22*, 524–532. [CrossRef]

27. Song, Z.; Yang, G.; Liu, X.; Yan, Z.; Yuan, Y.; Liao, Y. Comparison of Seven Chemical Pretreatments of Corn Straw for Improving Methane Yield by Anaerobic Digestion. *PLoS ONE* **2014**, *9*, e101617. [CrossRef] [PubMed]

28. Xiao, B.; Sun, X.; Sun, R. Chemical, Structural, and Thermal Characterizations of Alkali-Soluble Lignins and Hemicelluloses, and Cellulose from Maize Stems, Rye Straw, and Rice Straw. *Polym. Degrad. Stab.* **2001**, *74*, 307–319. [CrossRef]

29. Li, C.; Knierim, B.; Manisseri, C.; Arora, R.; Scheller, H.V.; Auer, M.; Vogel, K.P.; Simmons, B.A.; Singh, S. Comparison of Dilute Acid and Ionic Liquid Pretreatment of Switchgrass: Biomass Recalcitrance, Delignification and Enzymatic Saccharification. *Bioresour. Technol.* **2010**, *101*, 4900–4906. [CrossRef] [PubMed]

30. Ge, H.; Wang, C.; Liu, S.; Huang, Z. Synthesis of Citric Acid Functionalized Magnetic Graphene Oxide Coated Corn Straw for Methylene Blue Adsorption. *Bioresour. Technol.* **2016**, *221*, 419–429. [CrossRef] [PubMed]

31. Chatterjee, S.; Guha, N.; Krishnan, S.; Singh, A.K.; Mathur, P.; Rai, D.K. Selective and Recyclable Congo Red Dye Adsorption by Spherical Fe3O4 Nanoparticles Functionalized with 1,2,4,5-Benzenetetracarboxylic Acid. *Sci. Rep.* **2020**, *10*, 111. [CrossRef] [PubMed]

32. Meenakshisundaram, S.; Calcagno, V.; Ceballos, C.; Fayeulle, A.; Léonard, E.; Herledan, V.; Krafft, J.-M.; Millot, Y.; Liu, X.; Jolivalt, C.; et al. Chemically and Physically Pretreated Straw in Moderate Conditions: Poor Correlation between Biogas Production and Commonly Used Biomass Characterization. *Energies* **2023**, *16*, 1146. [CrossRef]

33. Nunes, C.S.; de Souza Castillo, A.; Ramos, J.P.; Gomes, L.G.; Cardoso, F.J.B.; do Socorro de Souza Vilhena, K. Potencial de Resíduo Não Processado Proveniente Da Obtenção Do Silício Metálico Como Adsorvente Do Corante Vermelho de Metila. *Matéria (Rio Janeiro)* **2023**, *28*. [CrossRef]

34. Almeida, C.A.P.; Machado, C.; Debacher, N.A. Adsorption of Methylene Blue as a Model for the Use of Barro Branco as an Alternative Adsorbent for Color Removal. *Surf. Colloid Sci.* **2004**, 278–282. [CrossRef]

35. Hu, Z.; Chen, H.; Ji, F.; Yuan, S. Removal of Congo Red from Aqueous Solution by Cattail Root. *J. Hazard. Mater.* **2010**, *173*, 292–297. [CrossRef]

36. Wang, G.; Chen, H. Fractionation of Alkali-Extracted Lignin from Steam-Exploded Stalk by Gradient Acid Precipitation. *Sep. Purif. Technol.* **2013**, *105*, 98–105. [CrossRef]

37. Wen, J.; Xue, Z.; Yin, X.; Wang, X. Insights into Aqueous Reduction of Cr(VI) by Biochar and Its Iron-Modified Counterpart in the Presence of Organic Acids. *Chemosphere* **2022**, *286*, 131918. [CrossRef]

38. Balbina, F.T.C.d.S. Fenômeno de Modulação Termo-Óptica Do Corante Azul de Metileno Utilizado Em Terapia Fotodinâmica. Ph.D. Thesis, Universidade Anhembi Morumbi, São Paulo, Brazil, 2023.

39. Toma, H.E.; da Silva Bonifácio, L.; Anaissi, F.J. Da Cor à Cor Inexistente: Uma Reflexão Sobre Espectros Eletrônicos e Efeitos Cromáticos. *Quim. Nova* **2005**, *28*, 897–900. [CrossRef]

40. Fernández-Pérez, A.; Marbán, G. Visible Light Spectroscopic Analysis of Methylene Blue in Water; What Comes after Dimer? *ACS Omega* **2020**, *5*, 29801–29815. [CrossRef]

41. The Dimensions of Colours. Available online: http://www.huevaluechroma.com/045.php (accessed on 24 January 2024).

42. Hirschler, R. Electronic Colour Communication in the Textile and Apparel Industry. *Redige Rev. Des. Innov. Strateg. Manag.* **2010**, *1*, 43–61.

43. Horsth, D.F.L.; Primo, J.O.; Dalpasquale, M.; Bittencourt, C.; Anaissi, F.J. Colored Aluminates Pigments Obtained from Metallic Aluminum Waste, an Opportunity in the Circular Economy. *Clean. Eng. Technol.* **2021**, *5*, 100313. [CrossRef]

44. Debrassi, A.; Largura, M.C.T.; Rodrigues, C.A. Adsorção Do Corante Vermelho Congo Por Derivados Da O-Carboximetilquitosana Hidrofobicamente Modificados. *Quim. Nova* **2011**, *34*, 764–770. [CrossRef]

45. de Oliveira, B.; Moriyama, L.; Bagnato, V. Colorimetric Analysis of Cotton Textile Bleaching through H2O2 Activated by UV Light. *J. Braz. Chem. Soc.* **2017**, *29*, 1360–1365. [CrossRef]

46. Beg, M.D.H.; Pickering, K.L.; Gauss, C. The Effects of Alkaline Digestion, Bleaching and Ultrasonication Treatment of Fibre on 3D Printed Harakeke Fibre Reinforced Polylactic Acid Composites. *Compos. Part A Appl. Sci. Manuf.* **2023**, *166*, 107384. [CrossRef]